

# An Autonomous Sensor with Energy Harvesting Capability for Airflow Speed Measurements

A. Flammini, D. Marioli, E. Sardini, M. Serpelloni

Department of Information Engineering

University of Brescia

V. Branze 38, 25123 Brescia, Italy

mauro.serpelloni@ing.unibs.it

**Abstract** — In several environments modest ambient airflows are present, for example, in air-conditioning ducts, in outdoor environment, or in moving vehicles. Furthermore, an airflow speed measurement is an important indicator, for the energy efficiency in the regulation of the conditioning implants. An autonomous sensor placed in a duct and powered by an electromechanical generator scavenging energy from the airflow has been designed and tested. The airflow speed is measured through the rotor frequency of the electromechanical generator. When the external readout unit is active the electromagnetic field is used to power the autonomous sensor system and transmit the data. A set of tests on three airflow harvesters using resistive loads was conducted to demonstrate their energy conversion potentials. An experimental system has been designed and realized demonstrating that the airflow harvester can power the autonomous sensor permitting airflow speed measurements.

**Keywords** - *Autonomous sensor; airflow measurement; telemetry; contactless system; power harvesting; energy scavenging, wind energy.*

## I. INTRODUCTION

Airflow measurements contribute to determine the indoor air quality and to provide healthy environments for the occupants of the buildings. They are also used for wind measurement in open space, in specific point sometimes difficultly accessible and without any availability of electricity. This paper outlines an airflow sensor that autonomously performs the measuring and saving functions, and transmits data to an external readout unit without requiring any battery. The autonomous sensor is powered by a harvesting system. Without batteries, the system has a positive ecological impact: no replacement costs or disposal problems. In addition the lack of batteries makes easier to measure at any point of a building or in places where there is no electricity. A growing demand for autonomous sensors and autonomous nodes is leading to a subsequent increase in the demand for localized, independent energy harvesting capabilities for each node or sensor [1, 2]. The use of power harvesting modules as a power source presents interesting possibilities, eliminating the batteries. In the literature, airflow harvesters are evaluated for their potential utilization in autonomous measurements. An airflow harvester can be a promising technological solution for producing electricity in remote applications [3-6]. In general, it is necessary for the power consumption of the harvesting electronics to be less than the available power for harvest,

which varies as a function of wind speed. In recent years, several groups have demonstrated small airflow harvesters based on the wind turbine principle. For this purpose, a properly sized small wind turbine is required to exploit the available wind potential for producing electrical energy. In [3], a wind energy system is evaluated for their potential utilization in urban areas. The techno-economic analysis of such energy systems is reported, as well as their life cycle assessment. In [7], the paper reports on the design, fabrication, and testing of small scale piezoelectric windmill. The windmill was tested at average wind speed of 4.47 m/s and it provided 5 mW continuous power. In [8], a 100 mm diameter fan rotor is combined with a brushless DC motor operated as a generator that could deliver up to 28 mW at 5.1 m/s flow rate or 8 mW at 2.5 m/s. More recently, in [9] a smaller device, with a 4.2-cm diameter rotor, is described. The device delivers powers of 2.4 and 130 mW at flow rates of 5.5 and 12 m/s, respectively. In [10] a small scale airflow harvester is reported. This device was developed using MEMS technology and was aimed at higher flow-rate applications. It comprises a 12-mm-diameter axial-flow turbine integrated with an axial-flux electromagnetic generator.

In this paper an autonomous sensor for measuring airflow speeds are presented. This autonomous sensor uses an airflow harvester for powering the sensor. A measure of flow is an important indicator of operational efficiency in the regulation of air conditioning, or in urban areas or in industrial implants [11, 12]. In the proposed application different airflow harvesters, using commercial rotor and generator parts, have been tested to study the power as a function of the load. An experimental setup has been arranged to test the autonomous sensor by measuring: the airflow speed inside a duct, voltage and current that can be generated by the airflow harvester. The applications here considered are those within a room or zone, such as through doorways (open or closed) or passive vents, those between the building and outdoors, and those through mechanical air distribution systems. For internal flow, such as ventilation ducts, the air speed can reach 12 m/s in large ducts, down to 1-2 m/s. For internal air duct applications, tiny windmills have significant advantages. Considering these aspects the autonomous sensor has been designed for low airflow speed.

## II. DESCRIPTION OF AUTONOMOUS SENSOR

In Figure 1, a schematic diagram of the autonomous sensor is shown. A commercial fan is connected to an electromagnetic generator. The power harvested, using the air motion energy, supplies an electronic circuit for the measurements of the same airflow. Therefore, when the autonomous sensor is placed in ducts and a sufficient airflow is present, the electromagnetic generator harvests energy, powering the electronic circuit. In this condition no external power source is necessary, the airflow measurement is performed and the data are saved into non-volatile memory. When necessary, these measurement data can be downloaded by an external unit placed close to the autonomous sensor. Since during this phase the autonomous sensor is supplied by an electromagnetic field generated by the external readout unit, the correct functioning is guaranteed even if no energy comes from the airflow power harvesting system.

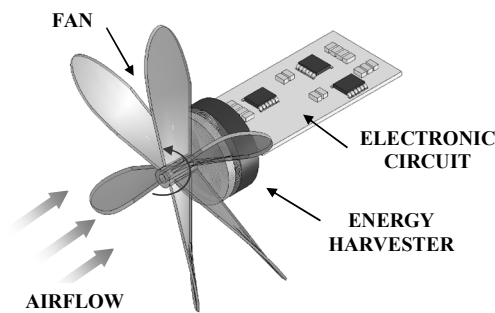


Figure 1. Schematic diagram of the autonomous sensor.

### A. Energy harvesters

Whereas the intent is to use the device indoors, in air ducts used for heating, ventilating, and air-conditioning, the airflow speed is used to drive a miniature electromagnetic wind turbine to harvest the energy. The adopted components for the airflow harvester are commercially available. Three different electromagnetic devices were tested to be adopted in the harvester: a brushless DC servomotor (AD0612 HB-C76GL Dr. Cooler), a brushless three phase AC servomotor (nuvoDisc 32BF Portescap) and a DC servomotor (1624T 1,4 G9 Faulhaber). The main features are reported in Table 1. The generators use a commercially available fan blade as a turbine blade (6 blades of 4 cm).

Table 1. Main features of the electromagnetic devices.

Company	Type	Dimension [mm]	Weight [g]
Dr. Cooler	brushless DC servomotor	27 x 27 x 15	22.7
Portescap	brushless 3-phase AC servomotor	16 x 16 x 33	30.8
Faulhaber	DC servomotor	32 x 32 x 22	35.9

### B. Electronic circuit

In Figure 2, the block diagram of the autonomous sensor and the readout unit are reported. The electronic circuit of the autonomous sensor consists of different modules. The transponder (U3280M) is commercialized by Atmel and its working frequency is 125 kHz. This device modulates the magnetic field by a damping stage to transmit data; in particular the OOK modulation and the Manchester code are chosen to modulate the signal. The transponder includes a power management block that handles the switching between the magnetic field and power harvesting supply. This component, able to supply the low-power microcontroller, consists of a rectifier stage for the antenna, a power manager, a damping modulator and a field-gap detection stage for RF communication. Therefore, the autonomous sensor provides the signal transmission through electromagnetic coupling at 125 kHz between the antenna of the transponder and the antenna of the readout unit. The advantage of transmitting an electromagnetic field at such comparatively low frequency is the possibility to more effectively transfer data and energy through different interposed materials without a cabled link. To transmit data, the transponder modulates the magnetic field using a damping stage. One pin of the device (clock extractor) is used to provide a clock signal for the synchronization of data transfer. The transponder interface can also receive data: the readout unit modulates the data with short gaps in the field and a gap-detection circuit reveals these gaps and decodes the signal. The autonomous sensor antenna has an inductance of about 640  $\mu$ H, while the readout antenna has a diameter of about 120 mm and an inductance of about 3.3 mH. Both are built by wrapped wire. The low-power microcontroller chosen is the 9S08QE128 commercialized from Freescale which offers an 8/12-bit analog to digital converter, 128 KB Flash memory to save the data and two timer units. The low-power microcontroller has a timer unit that permits to synchronize the data transmission. The microcontroller has a low-power configuration: all the unused peripherals are switched off. To maintain the power consumption low, the clock of the microcontroller is 500 kHz during the measurement and transmission, while the clock is 16.4 kHz during stop mode. The airflow speed is measured through the rotor frequency of the electromechanical generator using an infrared Light Emitting Diode (LED) and an NPN silicon phototransistor (Optek OPB815-WZ).

The readout unit consists of a transceiver (U2270B) commercialized by Atmel. This component permits to drive the coil antenna and to demodulate the digital signal. The transceiver is able to supply the transponder by generating a magnetic field through its antenna: a signal generator produces a sine wave voltage of up to 80 V<sub>pp</sub> at a frequency range of 125 kHz. The transceiver is connected to a microcontroller (9S08AW60) commercialized by Freescale. The readout unit is supplied by an external power. The operating voltage is 5 V and the frequency of the bus clock is 7.38 MHz. A timer unit is used to decode the demodulated signal and the data collected are transferred to a personal computer (PC) using a serial communication interface (SCI).

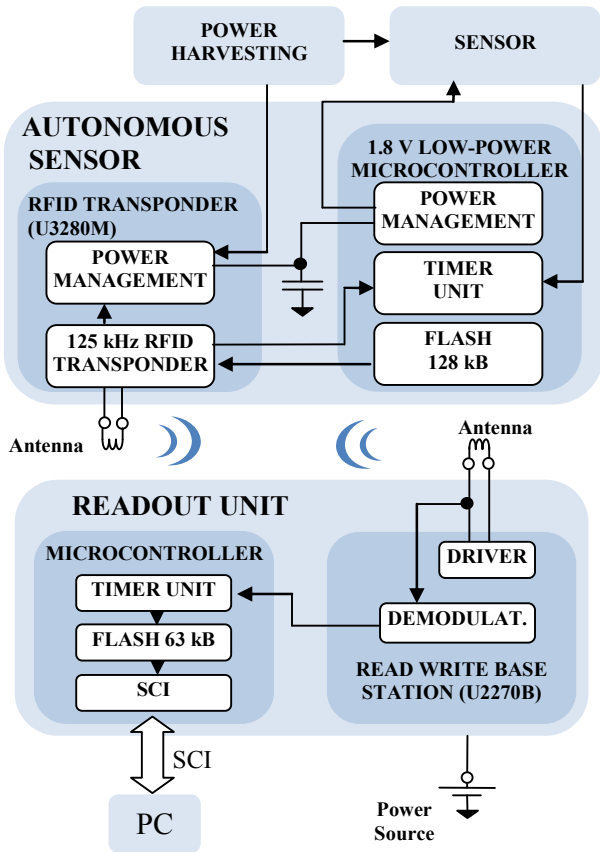


Figure 2. Block diagram of the autonomous sensor and readout system.

### III. EXPERIMENTAL SYSTEM

An experimental setup has been developed for the characterization of the power harvesters and the autonomous sensor. In Figure 3, the schematic diagram of the experimental system is shown.

The wind tunnel has been specially designed and developed in laboratory for system calibration purposes. The wind tunnel used has a 20 cm diameter test section with a settling chamber at the entrance and a length of 1 m. Air speed is measured using reference flowmeter (Lutron AM-4203), providing reading with an accuracy of  $\pm 2\%$  of the flow speed. The flowmeter is connected to the PC using the RS-232 cable.

A commercial airflow generator is used as source for the controlled airflow along the duct, while the airflow speed is monitored by the reference flowmeter. Full control on the air speed is possible, which allows tests from 0 up to 23 m/s. The rotational speed of airflow generator (24 V DC fan - Comair Rotron) is controlled by the PC: a programmable power supply (Agilent E3646A) supplies the airflow generator. The frequency output of the airflow generator is proportional to the 0–24 V DC input supply signal. The programmable power supply is connected by the GPIB cable to the PC, allowing the airflow generator to be driven by the virtual instrument. A

LabVIEW program controls the system, monitoring the airflow.

For the characterization of the energy harvesters two multimeters (Agilent 34401A) have been used for measuring voltage and current generated by the harvesters. All the tests were done at an ambient temperature of 20 °C and in the center of the tunnel. Therefore, to test the transmission activity the autonomous sensor has been located in the tunnel and communicates with the readout unit externally placed. The airflow speed data, collected by the autonomous sensor, are compared with the reference flowmeter (Lutron AM-4203). The signals at the antenna are controlled by an oscilloscope (LeCroy LT374M).

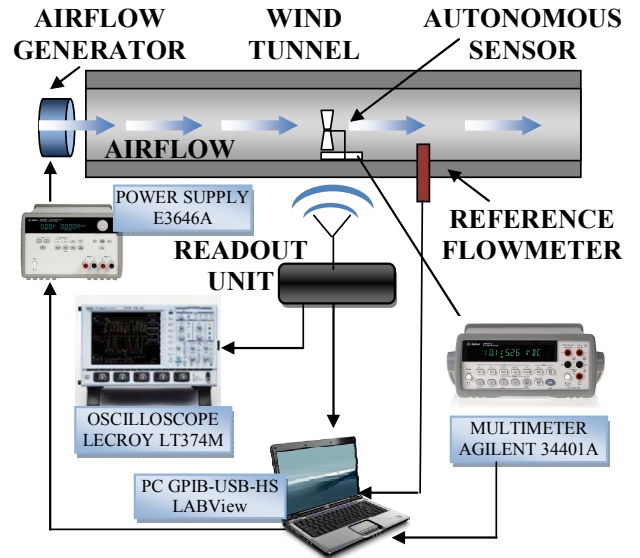


Figure 3. Schematic diagram of the experimental system.

### IV. CHARACTERIZATION OF THE ENERGY HARVESTERS

A set of tests on the airflow power harvesters using different resistive loads and airflow speeds to demonstrate their energy conversion potentials was conducted.

In the literature, the use of wind turbines or airflow harvesters to power autonomous sensors is reported [12]. The available theoretical airflow power can be calculated with the kinetic energy. Using the formula for the moving system, the flow energy can be obtained:

$$E = \frac{1}{2}mv^2 = \frac{1}{2}\rho A\Delta t v^3 \quad (1)$$

Where  $\rho$  is the fluid density,  $A$  is the area normal to flux,  $v$  is the airflow speed and  $\Delta t$  is the observation time and  $m$  the mass. The kinetic energy can be easily converted into the airflow power:

$$P_w = \frac{1}{2}\rho A v^3 \quad (2)$$

This power is function of air density, which can be assumed to be of 1.2 kg/m<sup>3</sup>, area and airflow speed.

The theoretical maximum quantity of energy for a standard area of 55 cm<sup>2</sup> and a wind velocity 4.5 m/s is about 300 mW. A generator module cannot extract all of this power, since the relatively high viscous drag on the blades, the bearing losses and other factors. The wind power is corrected with a power coefficient less than unity ( $C_p$ ). Large-scale airflow harvesters can be highly efficient, with power coefficients greater than 0.5 being achievable; for small-scale airflow harvesters the performance is less good, about 0.1 [4]. This large variation in efficiency is caused by friction in the generator, internal electric resistance and the power extracted.

The wind turbine is a well known device for extracting power from airflows on a large scale, and miniaturization of this device is a natural starting point for airflow harvesting on a smaller scale.

The power extracted by a practical turbine is

$$P_m = \frac{1}{2} C_p \rho A v^3 = C_p P_w \quad (3)$$

Where  $C_p$  is the power coefficient of the turbine.

Assuming that the turbine is coupled to a transmission with efficiency  $\eta_m$  which drives a generator of efficiency  $\eta_g$ , the electrical power  $P_e$  available can be written as:

$$P_e = \eta_m \eta_g C_p P_w \quad (4)$$

The energy harvester efficiency is defined as the power extracted from the airflow over the kinetic power available for the area covered by the disk of the fan. The maximum turbine efficiency increases with the tip speed ratio up to a maximum theoretical value of 59% (Betz limit). For small-scale airflow harvesters the performance is less good. This large variation in efficiency is caused, as specified before, by friction in the generator, internal electric resistance and the power extracted.

The generators (reported in Table 1) were analyzed measuring voltage and current for different airflow speeds and connected loads. The efficiency is calculated as ratio of measured power ( $P_e$ ) and the kinetic power ( $P_w$ ) calculated mathematically with (2) considering an area of about 28 cm<sup>2</sup>.

#### A. Brushless DC servomotor

In Figure 4, the power values generated using the brushless DC generator for different loads and different airflow velocities are reported.

Analyzing the diagrams, as expected, when the resistance is high there are low currents flowing to the load, which means zero efficiency, as all the mechanical energy goes in friction. On the other end, when the load is low, high current reduces the voltage across the generator, reducing the efficiency, as the power is dissipated as heat in the coils. Therefore, the diagrams have a maximum power of 16 mW, which can be observed for a load of 150  $\Omega$ . The maximum calculated efficiency is about 2 %.

The brushless DC servomotor can work correctly also for low airflow speeds considering that commercial boost converters can be used. These devices, used to step-up the voltage to supply the electronic circuit, have a minimum input voltage of about 0.6 mV.

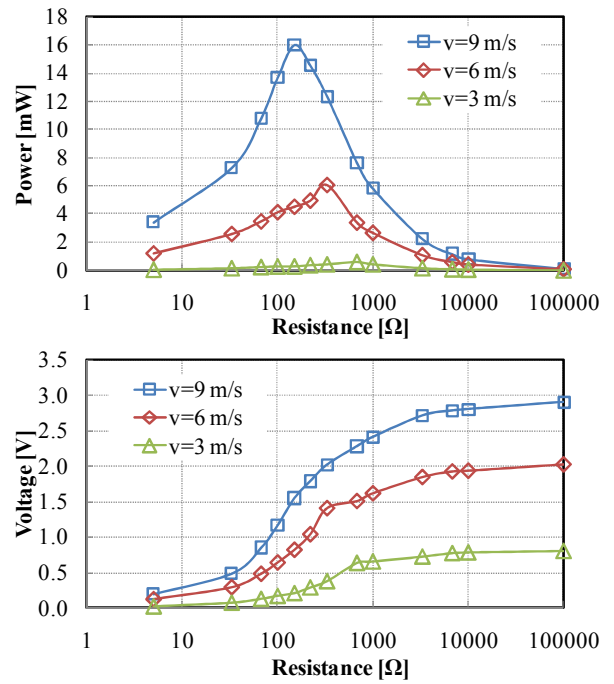


Figure 4. Generated power by the brushless DC servomotor at different airflow speeds.

#### B. DC servomotor

In Figure 5, the diagrams obtained for the DC servomotor are shown. Using the DC servomotor the maximum power extracted is about 35 mW for a load of 80  $\Omega$ . The maximum calculated efficiency is about 8 %. Furthermore, the voltages are higher than those of the previous case.

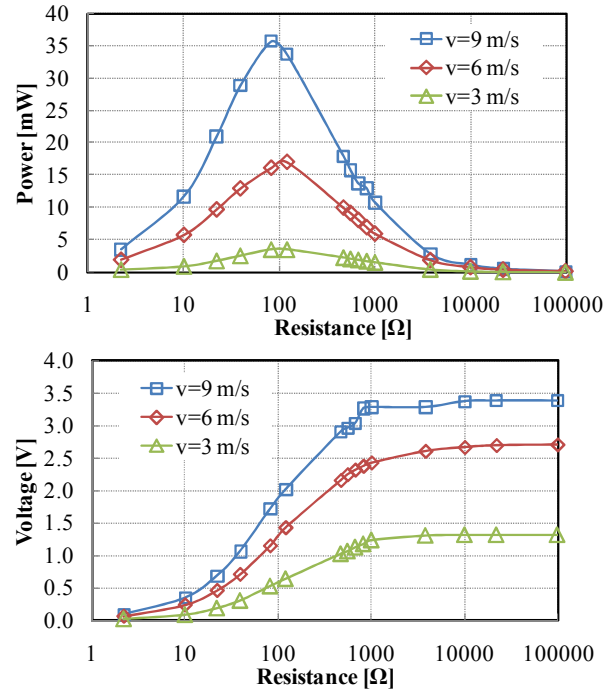


Figure 5. Generated power by the DC servomotor at different airflow speeds.

### C. Brushless three phase AC servomotor

In Figure 6 the experimental results obtained with the brushless three phase AC servomotor are reported.

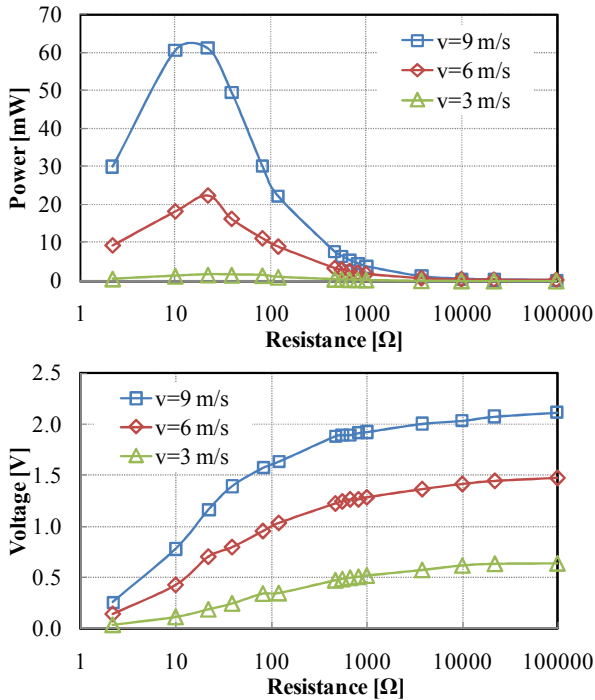


Figure 6. Generated power by brushless three phase AC servomotor at different airflow speeds.

In this case the RMS values of voltage and current are calculated using the sinusoidal measured signals. A maximum power of 60 mW can be observed for a load of 20 Ω. The maximum calculated efficiency is about 6 %. The AC power generator needs a rectifier that can simply be obtained by a bridge with diodes, but this stage reduces the total amount of energy disposable.

The maximum efficiencies calculated for the three harvesters are lower than 8 %. A factor contributing to the low efficiency is that the harvester uses a blade designed to operate as a fan at high speed, not at low airflow speed. The best opportunity to increase the efficiency could be using a better blade.

## V. CHARACTERIZATION OF THE AUTONOMOUS SENSOR

The activities of the autonomous sensor are schematized as stop, measuring and saving. When the readout unit is active there is the transmission of data. To characterize the correct functioning of the autonomous sensor, the power harvesters have been connected to the electronic circuit and the autonomous sensor has been tested in the wind tunnel. For the three-phase AC servomotor a three-phase bridge was constructed from six diodes (1PS74SB23) and used to convert the AC current from the motor to DC current required by the autonomous sensor (Figure 7). As expected the AC servomotor

do not present the best solution. A factor contributing a lower efficiency is the non-ideal characteristics of the diodes in the three-phase bridge circuit. The diodes do not conduct until they are forward-biased by 0.3 V, which is a significant fraction of the output of the bridge circuit.

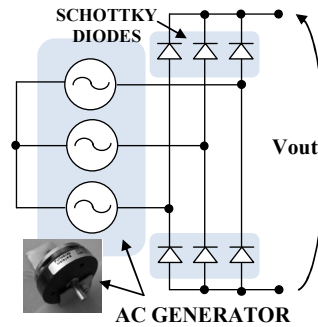


Figure 7. Frequency values vs. different airflow speeds.

For each harvester, voltage and current have been measured for different airflow speeds. In Figure 8 the experimental data are shown. As expected, the AC servomotor is less efficient than the others, due to the rectifier stage. For each curve a similar behavior in the results can be noticed: each curve shows, for a given value of speed, an initial increasing in power and then a decreasing. This behavior is due to a variation of the equivalent resistance of the electronic circuit during the starting phases. When the sensor is completely activated, it stands in a state of low-power and thereby the power consumption is reduced, allowing working even at lower values of speed. Subsequent tests were conducted using the DC servomotor.

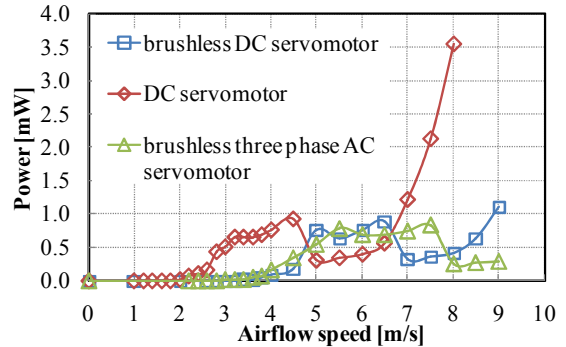


Figure 8. Frequency values vs. different airflow speeds.

The airflow speed is measured by the autonomous sensor measuring the rotation of the fan generator using the infrared Light Emitting Diode (LED) and an NPN silicon phototransistor (Optek OPB815-WZ), which are powered only during the measurement phase. The input capture characteristic of the microcontroller is adapted to measure the period between two consecutive passages of the blade and to calculate the rotation period. In Figure 9, the rotation frequency values are obtained using different airflow speeds. The black line represents the linear interpolation of the data.

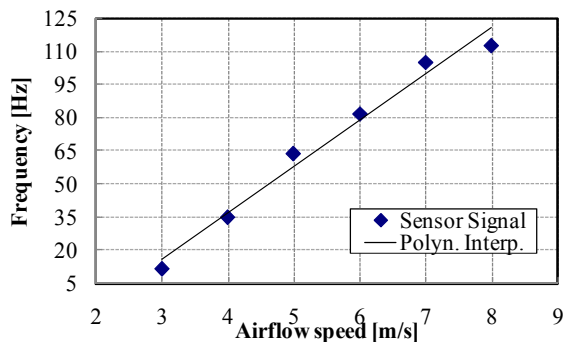


Figure 9. Frequency values vs. different airflow speeds.

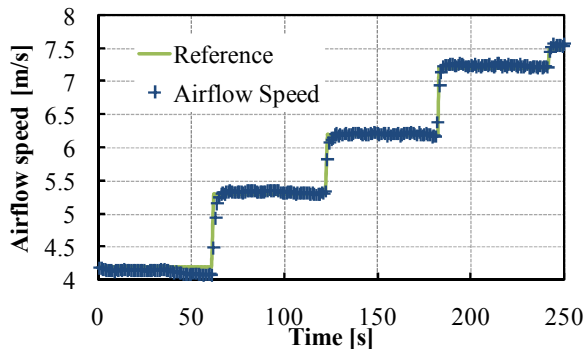


Figure 10. Calculated values of airflow speed compared with the values obtained with the reference flowmeter.

In Figure 10, the calculated values of airflow speeds compared with the values obtained with the reference flowmeter are reported. The system begins working for airflow speed higher than 4 m/s, but when active can also operate at speeds of 3 m/s. Subsequently, the measured data are stored into a non volatile memory and downloaded to the readout unit. Depending on the power supply of the airflow harvester, if the airflow is not sufficient to supply the autonomous sensor, this can generate a black-out period. For this reason it is not able to record a trace of an absolute time of the measurement.

## VI. CONCLUSIONS

This paper has demonstrated that airflow is a viable source of energy for powering autonomous sensors. At this purpose, an autonomous sensor has been developed for airflow speed measurements in ducts for civil or industrial applications. The results from testing the prototype indicate that, with careful

design of the airflow harvester, it is possible to supply the electronic circuit of the autonomous sensor. The preliminary experimental data show that is possible to operate at velocities as low as 4 m/s. The lower value of speed may be reduced by using a low-power sensor, for example capacitive, several studies are undertaken. A further reduction could be achieved if the electronics were developed ad hoc as IC and then removing that part of the electronic circuitry that is not necessary. Moreover, even if the autonomous sensor does not present the information of time, it is still able to detect whether the value of the flow exceeds a certain value and how many times does.

## REFERENCES

- [1] P. Nema, R.K. Nema, S. Rangnekar, A current and future state of art development of hybrid energy system using wind and PV-solar: A review. *Renewable, Sustainable Energy Reviews* 13 (2009), 2096–2103.
- [2] R. Morais, S.G. Matos, M.A. Fernandes, A.L.G. Valente, S.F.S.P. Soares, P.J.S.G. Ferreira, M.J.C.S. Reis, Sun, wind and water flow as energy supply for small stationary data acquisition platforms. *Computers and electronics in agriculture* 64 (2008), 120–132.
- [3] M.A. Weimer, T.S. Paing, R.A. Zane, Remote area wind energy harvesting for low-power autonomous sensors. *Power Electronics Specialists Conference*, 18(22), (2006), 1-5.
- [4] P.D. Mitcheson, E.M. Yeatman, G.K. Rao, A.S. Holmes, T.C. Green, Energy harvesting from human and machine motion for wireless electronic devices. *Proceedings of the IEEE* 96(9), (2008), 1457-1486.
- [5] H.J. Jung, S.W. Lee, D.D. Jang, Feasibility Study on a New Energy Harvesting Electromagnetic Device Using Aerodynamic Instability Magnetics. *IEEE Transactions on*, 45 (2009), 4376 – 4379.
- [6] C. Vlad, I. Munteanu, A.I. Bratcu, E. Ceanga, Output power maximization of low-power wind energy conversion systems revisited: Possible control solutions. *Energy Conversion and Management* 51 (2010), 305–310.
- [7] R. Myers, M. Vickers, H. Kim, Small scale windmill. *Appl. Phys. Lett.*, 90, (2007), paper 054 106.
- [8] C.C. Federspiel, J. Chen, Air-powered sensor. *Proc. IEEE Sensors*, 1, (2003), 22–25.
- [9] D. Rancourt, A. Tabesh, L. G. Frechette, Evaluation of centimeter-scale micro wind mills: Aerodynamics and electromagnetic power generation. *Proc. PowerMEMS*, Freiburg, Germany, (2007), 93–96.
- [10] A.S. Holmes, G. Hong, K.R. Pullen, Axial-Flux Permanent Magnet Machines for Micropower Generation. *Journal of microelectromechanical systems*, 14(1), (2005), 54-62.
- [11] A.N. Celik, T. Muneer, P. Clarke, An investigation into micro wind energy systems for their utilization in urban areas and their life cycle assessment. *Proc. IMechE 221 Part A: J. Power and Energy*, (2007), 1107-1117.
- [12] F. L. Peña, R. J. Duro, A Virtual Instrument for Automatic Anemometer Calibration with ANN Based Supervision. *IEEE Transactions on Instrumentation and Measurement*, 52(3), (2009), 654 - 661.